Chalcogenide Letters Vol. 21, No. 4, April 2024, p. 319 - 326

Investigation and structural of phosphate glasses at low photon energy through: optical and attenuation properties

L. Alelyani[a], T. A. Ghawa[b,*], N. A. Asiri[b], N. A. Abdullah[b], K. I. Hussein[b], M. S. Alqahtani[b]
[a]*Department of Physics, Ministry of Education, Riyadh, Saudi Arabia.*
[b]*Department of Radiological Sciences, College of Applied Medical Sciences, King Khalid University, Abha 61421, Saudi Arabia*

This paper presents a novel low-cost phosphate glass preparation by using the melt quenching technique. It was investigated for use in diagnostic protective applications. The range of UV-VIS wavelength is used to estimate the optical energy gap. The MAC denotes the mass attenuation coefficients of the present glass were computed at low photon energies between 15 and 200 KeV using the MIKE program. The manufactured glasses parameters viz; the mean free path, half value layer, tenth value layer, effective atomic number, effective electron density, and linear attenuation coefficient denotes as follows; $MFP, HVL, TVL,\ Z_{eff}, N_{eff}, and\ LAC$ were determined. Furthermore, the molar volume, oxygen molar volume, and optical packing density of fabricated glass were assessed. The third-order susceptibility ($\chi^{(3)}$) and non-linear refractive index of the present glass were determined. From previous results, it can be concluded that the glass has unique attenuation characteristics, therefore, can be used for radiation protection at low energy 15 to 200 KeV.

(Received January 30, 2024; Accepted April 11, 2024)

Keywords: Phosphate, Nonlinear refractive index, Energy gap, Optical density, Polarizability, Half value layer, Mass attenuation coefficient, Half value layer

1. Introduction

Glass is one of the important radiation protection tools that prevents biologically deterministic effects and reduces the possibility of initiating stochastic effects in workers, patients, and staff [1]. This is under (ALARA) principle "as low as reasonably achievable", which is applied to reduce the amount of radiation exposure that uses radiation sources. Apart from reducing the exposure duration at the maximum practicable distance from the radiation source, it is also important to take into account the best available shielding techniques [2]. Lead (Pb) glass is normally used for radiation shielding. However, Pb has a high toxicity level and weak material properties, which may adversely affect human health and the environment. A recent trend has been to investigate the properties of glass, including transparency, cost-effectiveness, and ease of versatility in manufacturing [3].

Phosphate glass based on P_2O_5 exhibits many desirable properties, including low glass transition temperatures, low optical dispersions, high refractive indices, excellent thermal stability, strong transmission of infrared light within a broad wavelength range, and low phonon energy [4]. Moreover, these properties of phosphate glass are enhanced by the addition of heavy oxides BaO into the glass structure. Besides that, the presence of zinc oxide (ZnO) as a network modifier in the phosphate glass develops the thermal stability of glass, decreases the melting point and low crystallization rates, and lowers its chemical durability [5]. On the other hand, barium oxide (BaO) leads to improve the shielding features by increasing the mass attenuation coefficient, and density and also reduces secondary scattered radiation. It can enhance the absorption of ionizing radiation and improve the thermal properties of phosphate glasses. Thus, the purpose of this study is to analyze P_2O_5-ZnO-BaO glass systems' radiation

*Corresponding author: thekraasg30@hotmail.com
https://doi.org/10.15251/CL.2024.214.319

shielding properties between 15 and 200 KeV. The MIKE software [1- 3] was used to calculate various optical and radiation parameters, including the energy gap, nonlinear refractive index, polarizability, *MAC, LAC, HVL, MFP, N_{eff} and Z_{eff}.* Additionally, these results were computed to evaluate the created glass system's diagnostic shielding capabilities in comparison to a few commercially available standard materials for the creation of a new glass with lead-free shielding components.

2. Materials synthesis, theory and measurements

2.1. Preparation materials and UV-VIS-NIR spectroscopy

Using the melt quenching process, a glass sample was made with a composition of $0.5P_2O_5$-0.3ZnO- 0.2BaO (PZB) in mol%. After being heated in a furnace at temperatures 1200 °C for 30 minutes (depending on the composition), the mixing materials are put in a Pt crucible. Once the melt reached a high viscosity, it was stirred and then cast in a brass mold. It was annealed in a furnace at 420 °C for two hours. We identified the optical absorption spectra in the 200-2500 nm area using the UV-VIS-NIR spectrophotometer (JASCO V-570).

2.2.1. Density and physical parameters

The value of density is one of the critical parameters for material technology and its application which effects on mass absorption coefficient (μ_m).

The physical characteristics, including oxygen molar volume (V_o), oxygen packing density, O.p.d.,and molar volume (V_m), of fabricated glass are obtained by equation (1) [3-7]:

$$V_m = \frac{x_i m_i}{\rho}, \quad V_o = V_m.\left(\frac{1}{X_i N_i}\right), \; O.p.d = 1000.\frac{\rho \sum X_i N_i}{\sum X_i M_i} \tag{1}$$

Where, (x_i, m_i, n_i) represents the molecular weight of the glassy structure, the number of oxygen atoms in each oxide, and the molar proportion of each oxide compound in the glass composition. Therefore, we used equation (2) [4,5] to compute the molar refraction (R_m), molar polarizability (α_m)), and the metallization criteria (M_c):

where, (x_i, m_i, n_i) is the molar fraction of every oxide compound, the molecular weight of the glassy structure, and the number of oxygen atom of each oxide in the glass composition.

The molar refraction (R_m) molar polarizability (α_m), and the metallization criterion (M_c) can be calculated by using equation (2) [4,5]:

$$R_m = V_m.\left(\frac{n^2-1}{n^2+2}\right), \alpha_m = \frac{\pi}{4\pi N_A V_m}.\left(\frac{n^2-1}{n^2+2}\right), M_c = 1 - \frac{n^2-1}{n^2+2}. \tag{2}$$

where, N_A, is Avogadro's number and n is the linear refractive index. The linear susceptibility ($\chi^{(1)}$), nonlinear refractive index (n_2), and third-order nonlinear susceptibility ($\chi^{(3)}$) were obtained as follow [6];

$$\chi^{(1)} = \frac{(n^2-1)}{12.56}, n_2 = \frac{12\pi\,\chi^{(3)}}{n}, \chi^{(3)} = 1.7\left[\chi^{(1)}\right]^4 \times 10^{-10} \tag{3}$$

2.3. Radiation attenuation performance

To assess the effectiveness of certain materials for radiation shielding, different factors must be calculated. A linear attenuation coefficient LAC (μ) indicates with a given material thickness, x, the ratio of monoenergetic photons attenuated as described by Beer-Lambert equation [7]:

$$I = I_0 e^{-\mu X}$$
$$\mu = \text{LAC} = -\frac{\ln\frac{I}{I_0}}{X} \quad (4)$$

where, I, denotes the attenuated intensity of the photon beam in the interaction media and I_0, the unattenuated intensity of the photon beam. A measure of mass attenuation, MAC is physical quantities that measure the permeation of ionizing radiation through a material. The MAC can be calculated using the following equation (5):

$$\text{MAC} = \mu m = \frac{\mu}{\rho} = \sum wi \left(\frac{\mu}{\rho}\right)_i \quad (5)$$

where w_i indicates the fractional weight and $\left(\frac{\mu}{\rho}\right)_i$ the MAC of the individual component of each component, and the density of attenuated material.

Half-value attenuation of ionizing photons (HVL) is an important radiation shielding property that can be used to provide accurate measurements of the required shielding thickness. The HVL is calculated by the following equation (6):

$$\text{HVL} = \frac{0.693}{\text{LAC}} \quad (6)$$

Tenth-value layers TVLs represent the thickness of matter that minimize incoming radiation by tenth of its intensity. The TVLs are calculated by following equation (7):

$$\text{TVL} = \frac{2.3}{\text{LAC}} \quad (7)$$

The mean free path (MFP) of a single particle displays the typical distance it has traveled prior to they interact with the material. MFP is extremely important in determining radiation shielding performance. The MFP are calculated by following equation [8]:

$$\text{MFP} = \frac{1}{\text{LAC}} \quad (8)$$

An effective electron density N_{eff} and effective atomic number Z_{eff} are important factors in radiation shielding materials. The Z_{eff} are calculated by following equation (9):

$$Z_{eff} = \frac{\sum_i f_i A_i \left(\frac{\mu}{\rho}\right)_i}{\sum_j f_j \frac{A_j}{z_j} \left(\frac{\mu}{\rho}\right)_j} \quad (9)$$

Where, f_i, is the ith atomic element of the mole fraction, A_i, is its atomic weight, and , Z_j, is its atomic number.

N_{eff} is the number of electrons in each unit mass, a strong relationship exists between N_{eff} and Z_{eff}, which is calculated by following equation [10]:

$$N_{eff} = \frac{(\mu/\rho)}{\sigma_t} = \frac{N_A}{M} Z_{eff} \sum_i n_i = \frac{N_A Z_{eff}}{A} \quad (10)$$

where N_A, M and $\sum_i n_i$ are the Avogadro number, the total number of compound elements and molecular weight of the radiation shielding materials, respectively

3. Results and discussion

3.1. Optical investigations

All of these factors, V_m, V_0 and O.p.d. were taken into account when assessing the fragility or density of the prepared glass, and the results are shown in Table 1. ZnO ions were added to the P_2O_5-BaO glass matrix, resulting in a density value (=3.2857 $gm.cm^{-3}$) and an O.p.d. value of 78.2 gm.atm.L^{-1}. Herein we computed the value of, V_m, and V_o, which are equal to 38.363 and 12.788 cm^3, respectively, which represents distributions of oxygen in the glass matrix, are shown in Table 1. Changes in, V_m, and V_o are influenced by a variety of factors, including; First, the molecular weight of the components which make form the glass composition; Second, the number of oxygen atoms and length of the bond; Third, the radius of the cations; and fourth, the coordination number. They are important to take this into account when analyzing variations in the, V_m and V_o values. The density of crosslinks in the glass composition, coordination numbers with interstitial spaces, and the molecular weight of the glass constitution are important parameters that affect the density value in produced glasses, which is linked to structural changes in the glass.

Table 1. Sample code, density (ρ), molar volume (V_m), oxygen volume (V_o)and oxygen packing density ($O.P.D$).

Sample code	$\boldsymbol{\rho}$ (g/$\mathbf{cm^3}$)	$\boldsymbol{V_m(cm^3.mol^{-1})}$	$\boldsymbol{V_o(cm^3.mol^{-1})}$	$\boldsymbol{O.P.D(mol^{-1}}$
PZB	3.2857	38.363	12.788	78.2

Several variables affect the refractive index: (i) the quantity of doping ions' coordination, (ii) the anion's polarizability, (iii) the density of the materials used, and (vi) the bulk glasses optical basicity. Utilizing Eq. (2, 3), the metallization criteria (M_c), molar polarizability (α_m), and molar refraction (R_m) of the produced samples were determined. Therefore, the values of (R_m) and (α_m) values are 22.522 $cm^3.mol^{-1}$ and 9.937 $Å^3$, respectively. The value Mc, is equal 0.413, linear refractive index, n2, third order susceptibility, $\chi^{(3)}$, are equal 3.713$\times 10^{-11}$ and 2.261 10^{-12}esu, respectively, these results are shown in Table (2).

Table 2. Energy gap, E_{opt}, in eV, nonlinear refractive index (n_2) and third-order nonlinear susceptibility ($\chi^{(3)}$).

Sample code	E_{opt}, in eV	R_m $\boldsymbol{cm^3.mol^{-1}}$	α_m in $Å^3$	M_e	$\chi^{(3)}$ $\times \mathbf{10^{-12}}$esu	n_2 $\times \mathbf{10^{-11}}$esu
PZB	3.41	22.522	9.937	0.413	2.261	3.713

The absorption coefficient can be investigated by the following equation [11]:

$$\alpha = \frac{A}{d} \tag{11}$$

where (A) is the absorbance and (d) is the sample thickness. Investigation of absorption coefficient was carried out in order to determine the optical band gap (E_{opt}) [12]. For an indirect

transition the optical absorption coefficient (α) and photon energy($h\nu$) can be used to determine E_{opt} by equation (12) which derived by Mott and Davis the following equation [6].

$$\alpha = \frac{B(h\nu - E_{opt})^r}{h\nu} \tag{12}$$

where B: is a constant, h: is the Plank's constant, ν: is the frequency, E_{opt} is the optical band gap r: is a constant describing the transition process [7]. Moreover, r is describing the transition process. n value is equal to 2 in case of direct allowed transition. While, if r equal to 1/2, it is related to indirect allowed transition. Consequently, the optical band gap is calculated and it's equal to 3.4 eV for PZB

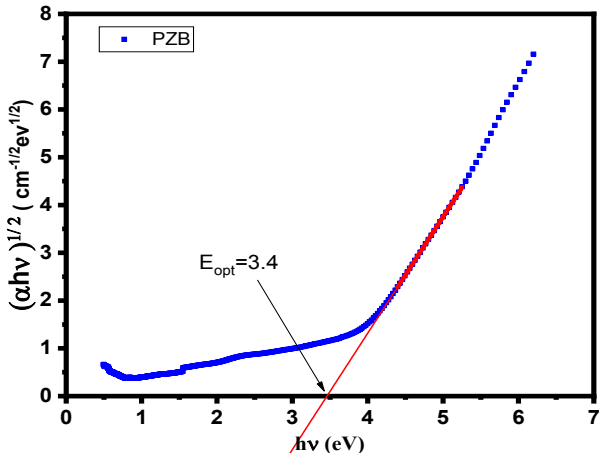

Fig. 1. For the prepared glass samples, the dependency of $(\alpha h\nu)^{1/2}$ *on the photon energy (hυ).*

3.2. Radiation shielding investigation

We calculated the shielding material properties for both standard and manufactured glass using monoenergetic gamma rays with energies ranging from 15 to 200 KeV. Figure 1a shows the mass attenuation coefficient MAC for each shielding material. The linear attenuation coefficient (LAC) for each shielding material is shown in Figure 1b; the LAC of materials decreases as the rate of energy increases. LAC is affected by density. A prominent peak at 0.1 MeV appears in the curve of the LAC measurement when samples are exposed to a low absorption edge.

When low-energy gamma photons are incident on samples, LAC and MAC values gradually decrease as a result of photoelectric interactions. The values of MAC and LAC gradually decreased as a result of Compton scattering at gamma photon energies (80– 900KeV), which has a clear relationship with both the photon energy and the square of the atomic number [11–13]. When the interaction between incoming photons and samples becomes closer to the pair formation zone at gamma photons higher, MAC and LAC values gradually grow. This relationship is exactly proportional to the square of the atomic number and directly proportional to the photon energy [29]. Additionally, as shown in Figures 2a and 2b, the linear attenuation of the produced glasses was compared to that of a few widely used standard radiation shielding materials, including RS–253 G18, RS–360, and RS–520 [8], at photon energies of 15 to 200 KeV.

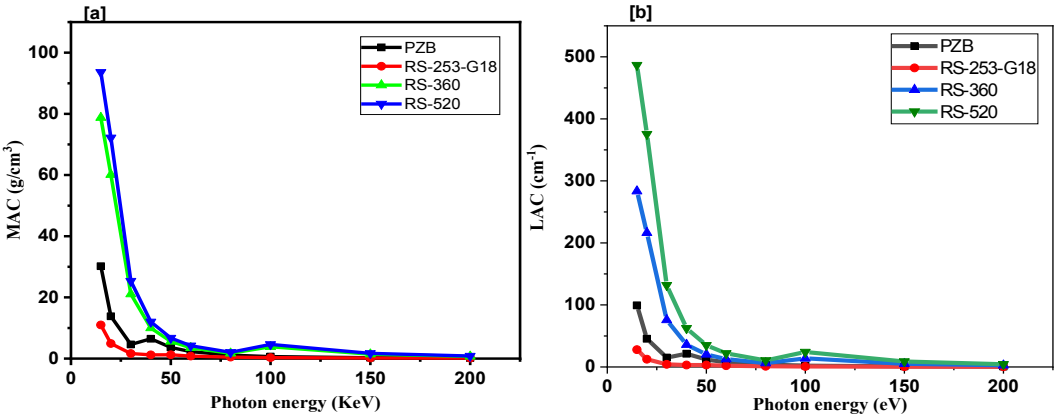

Fig. 2. (a) The glasses' mass attenuation coefficients in the energy range of 15-200 keV, (b) Linear attenuation coefficients of the glass in the energy range 15-200KeV.

For low-energy gamma photons, the values of HVL and MFP indicate the lowest values. These values gradually increase as photon energy increases until reaching approximately 200 KeV (see Figure 3), after which the values begin to remain nearly constant. HVL and MFP values are affected differently by photon energy interactions in different energy regions for prepared glass systems. Because of its low HVL value and high density of 3.2857 g/cm^3, fabricated glass can attenuate more ionizing radiation. When manufactured $0.5P_2O_5$-0.3ZnO-0.2BaO glass systems are compared to certain widely used standard radiation shielding materials coded RS–253 G18, RS–360, and RS–520, it is clear that the glass samples have superior characteristics, particularly at low photon energy.

On the other hand, Figure 4 indicate the MFP values of the prepared glass where they were comparable to the other radiation shielding materials at different gamma energies. The values recorded for the MFP also indicating the effectiveness of the prepared glasses. These results indicate that the prepared glasses recorded lower values compared to the standard materials, which means they have more shielding effectiveness.

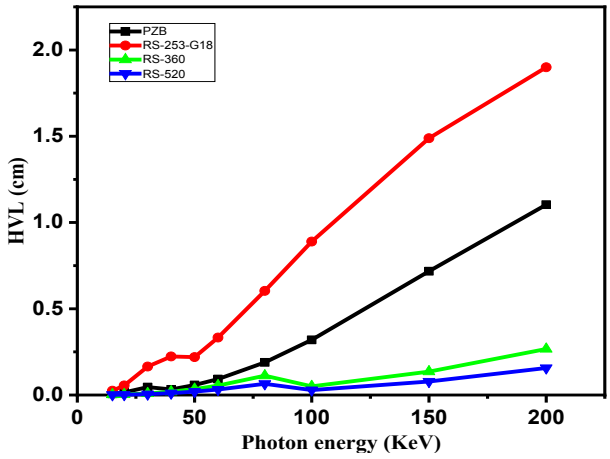

Fig. 3. Half value layer (HVL) values of the glass in the energy range 15-200KeV.

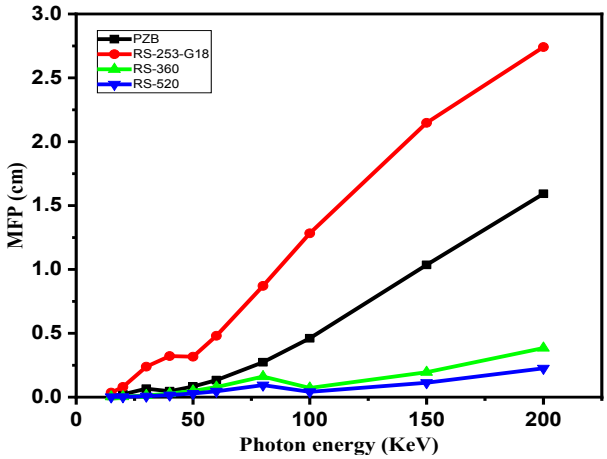

Fig. 4. In the energy range of 15-200KeV, the mean free path (MFP) values of the glass are investigated

Several types of materials are described using effective electron and atomic numbers N_{eff} and Z_{eff}. By studying the energy-dependent values of Z_{eff} and N_{eff}, one may get an extensive understanding of the behavior of the material when exposed to ionizing radiation [13].

The calculated Z_{eff} and N_{eff} values for the prepared glass samples were the highest and lowest at 15 and 200 KeV, respectively, as shown in Table 3, it can be assumed that the incident photon energy influences photoelectric, Compton and pair production processes. Z_{eff} and N_{eff} values are strongly influenced by incident photon energy. Photoelectric interactions result in a significant decrease in Zeff and Neff values as energy levels decreasing. During the medium energy regions, the Compton scattering effect causes them to remain in a relatively constant state, but they gradually increase at the higher energy levels due to pair production.

Table 3. Linear (LAC), mass attenuation coefficients, MAC, half value layer (HVL), mean free path (MFP) values, an effective electron density N_{eff} and effective atomic number Z_{eff} of fabricated glass at range 15 -200 KeV.

Photon Energy (keV)	LAC cm^{-1}	MAC cm^2/g	HVL cm	TVL cm	MFP cm	Z_{eff}	$N_{eff} \times 10^{+23}$
15	99.23583	30.20234	0.006983	0.023177	0.010077	31.51582	6.78
20	45.45466	13.83409	0.015246	0.0506	0.022	31.72069	6.82
30	15.10661	4.597683	0.045874	0.152251	0.066196	31.28155	6.73
40	21.31965	6.488617	0.032505	0.107882	0.046905	43.52148	9.36
50	12.01496	3.656742	0.057678	0.191428	0.08323	42.09703	9.05
60	7.51365	2.286773	0.092232	0.30611	0.133091	40.08743	8.62
80	3.662534	1.114689	0.189213	0.627981	0.273035	35.32308	7.59
100	0.660531	0.660531	0.31931	1.059758	0.460764	30.64063	6.59
150	0.293979	0.293979	0.717445	2.107999	1.035274	23.68606	5.09
200	0.191115	0.191115	1.103598	2.38113	1.592493	22.46961	4.83

4. Conclusions

The present study is focused on investigating the structural, physical, and optical properties of novel phosphate glasses. The determined density of the synthesized glasses was 3.2857 m/cm^3. The indirect optical energy (E_{opt}) band gaps 3.4 eV. The radiation shielding properties such as; $LAC, Z_{eff}, N_{eff}, HVL, TVL,\ and\ MFP$ equal 99.23583, 30.20234, 0.006983, 0.023177, 0.010077, 31.51582 and 6.78. at 15 KeV respectively. The present glass exhibited good optical properties which high n_2 ($3.713\times 10^{-11} esu$) and third order nonlinearity 2.261 10^{-12}esu. It concludes that glass can be used as candidate of X-ray shielding especially at 30 KeV.

Acknowledgments

The authors extend their appreciation to the Deanship of Scientific Research at King Khalid University, Saudi Arabia for funding this work through Large Research Groups Program under grant number RGP2/590/44.

References

[1] El S. Yousef, M. M. Elokr, Y. M. Aboudeif, Chalcogenide Letters 12, 597 (2015).

[2] A. M. Emara, M. M. Alqahtani, Y. M. Abou Deif , El Sayed Yousef, Chalcogenide Letters 14, No. 9, 405, (2017).

[3] Y. M. Aboudeif, M. M. Alqahtani, A. M. Emara, H. Algarni, El S. Yousef, Chalcogenide Letters 15, 219 (2018).

[4] K. I. Hussein, M. S. Alqahtani, A. Almarhaby, R. S. Alayyash, E. ElshiekhJournal of Ovonic Research Vol. 19, No. 2, March - April 2023, p. 141 – 151; https://doi.org/10.15251/JOR.2023.192.141

[5] A. M. Alqahtani, M. S. Alqahtanib, K. I. Hussein, A. J. Alkulib,F. F. Alqahtani, N. Elkhoshkhany, I. S. Yaha, M. Reben, E. Yousef, Chalcogenide Letters Vol. 19, No. 4, April 2022, p. 227 - 239.

[6] A. Z. Alzuhaira, M. S. Alqahtania, A. J. Alkuliba, K. I. Hussein, M. Reben, E. Yousef, Chalcogenide Letters Vol. 19, No. 3, 2022, 187- 195; https://doi.org/10.15251/CL.2022.193.187

[7] A. M. Alqahtani, M. S. Alqahtani, K. I. Hussein, A. J. Alkulib, F.F. Alqahtani, E.Yousef, Chalcogenide Letters Vol. 18, No. 9, September 2021, p. 513 – 523; https://doi.org/10.15251/CL.2021.189.513

[8] A. M. Al-Syad, M. Alfarh, H. Algarni, M. S. Alqahtani, M. Reben, H. Afifi, El Sayed Yousef, Chalcogenide Letters, Vol. 18, No. 9, September 2021, p. 541 - 54

[9] E.E. Assem, I. Elmehasseb, J. Mater. Sci. 46 (7) (2011) 2071-2076; https://doi.org/10.1007/s10853-010-5040-0

[10] N. Elkhoshkhany, Ola Essam, Amira M. Embaby, Chem. Phys. 214 (2018) 489-498; https://doi.org/10.1016/j.matchemphys.2018.05.007

[11] M.H.A. Mhareb, Muna Alqahtani, Fatimh Alshahri, Y.S.M. Alajerami, Noha Saleh, N. Alonizan, M.I. Sayyed, et al., J. Non. Solids 541 (2020), 120090; https://doi.org/10.1016/j.jnoncrysol.2020.120090

[12] P. Kaur, et al., Spectro. Acta Part A: Molecu. Biomolec. Spectro. 206 (2019) 367-377; https://doi.org/10.1016/j.saa.2018.08.038

[13] Y. M. AbouDeif, M. Reben, E. S. Yousef, A. E. Al-Salami, A. S. Al Shehri, Journal of Nanoelectronics and Optoelectronics, 14(4), (2019) 448-455; https://doi.org/10.1166/jno.2019.2585